Solar Energy Materials and Solar Cells 200 (2019) 109970

Contents lists available at ScienceDirect

Solar Energy Materials and Solar Cells

journal homepage: www.elsevier.com/locate/solmat

Easy-to-apply methodology to measure the hydrogen concentration in boron-doped crystalline silicon

Dominic C. Walter[a,*], Dennis Bredemeier[a,d], Robert Falster[b], Vladimir V. Voronkov[c], Jan Schmidt[a,d]

[a] Institute for Solar Energy Research Hamelin (ISFH), Am Ohrberg 1, 31860, Emmerthal, Germany
[b] 4 Harrison's Lane, Woodstock, OX20 1SS, UK
[c] Global Wafers, Via Nazionale 59, 39012, Merano, Italy
[d] Department of Solar Energy, Institute of Solid-State Physics, Leibniz University Hannover, Appelstr. 2, 30167, Hannover, Germany

ARTICLE INFO

Keywords:
Crystalline silicon
Hydrogen
Boron-hydrogen-pairs

ABSTRACT

Hydrogen is a highly relevant impurity in crystalline silicon associated with a variety of effects particularly important in solar cell technology such as defect and surface passivation. It has been the subject of countless studies. Much of this however relies to a certain degree on speculation due to limitations in hydrogen measurement capability, making a direct quantitative correlation of these phenomena with the hydrogen content largely impossible so far. In this contribution, we apply recent advances in the understanding of hydrogen introduction and behaviour in silicon - in particular the conversion of quenched in dimeric hydrogen to boron hydrogen pairs (BH) - and introduce an easy-to-apply methodology to determine quantitatively the hydrogen concentration in bulk boron-doped silicon. The technique involves the measurement and analysis of changes to the bulk resistivity, as recorded by contactless eddy-current measurements, due to the formation of BH pairs during annealing at temperatures between 140 and 180 °C. To demonstrate the method, we apply it to boron-doped float-zone silicon wafers with SiN_x:H coatings of different compositions, introducing different total hydrogen concentrations between 5×10^{14} and $1.3 \times 10^{15}\,cm^{-3}$ into the silicon bulk during a fast-firing step. Without firing, the hydrogen content is below the detection limit of $3 \times 10^{14}\,cm^{-3}$ for the 1 Ω cm test sample used.

1. Introduction

The properties of hydrogen in crystalline silicon has attracted the attention of many research groups world-wide over the past years, as it plays an important role in certain technologically relevant effects such as the passivation of surfaces and bulk defects [1–7]. Up to now, however, a major issue of these studies was that a quantitative measure of the absolute hydrogen concentration within the silicon bulk was practically inaccessible. Measurements of the absolute hydrogen content using e.g. secondary ion mass spectrometry (SIMS) [8] or low temperature Fourier-transformed spectrometry [9] are in principle applicable, but are rather difficult, as very low detection limits have to be achieved, or rely on intentional contamination [2]. An easy-to-apply methodology to determine the hydrogen concentration in the silicon bulk under relevant conditions would thus be very helpful to evaluate, for example, how much hydrogen is introduced in typical solar cell production processes and to learn how to modify those processes and effectively design them to control the amount of hydrogen incorporated.

Within this study, we introduce a simple methodology to measure the hydrogen content in boron-doped crystalline silicon. By annealing the silicon sample, some of the hydrogen, which is originally present in the form of hydrogen dimers, is transferred into boron-hydrogen (BH) pairs. The hydrogen passivation of dopant atoms leads to a corresponding increase of the wafer resistivity, which is recorded using contactless eddy-current measurements. For the quantitative evaluation of our measurement data, we apply a model developed by Voronkov and Falster [10], which includes the formation and dissociation of different kinds of hydrogen dimers in crystalline silicon as well as the formation of BH pairs [11–13]. By fitting the model to the measured resistivity changes, the absolute hydrogen concentration is determined. Here, in the first application of the new technique, we present various examples of samples featuring different silicon nitride layers, which introduce different amounts of hydrogen into the silicon bulk and ask

* Corresponding author.
E-mail address: d.walter@isfh.de (D.C. Walter).

https://doi.org/10.1016/j.solmat.2019.109970
Received 5 April 2019; Received in revised form 24 May 2019; Accepted 24 May 2019
Available online 30 May 2019

Table 1
Properties of the SiN_x:H layers investigated within this study. Thickness and refractive index are determined via ellipsometry measurements, the hydrogen concentration of the SiN_x:H layers is determined via FTIR measurements.

	Thickness [nm]	Hydrogen concentration [$\%_{at.}$]	Refractive index *n*
SiN_x:H-1	100	10	2.4
SiN_x:H-2	70	12	2.1
SiN_x:H-3	100	13	2.5

the question whether or not the known hydrogen content of the film is an indicator of subsequent hydrogen concentration incorporated in the bulk following firing.

2. Experimental details

The samples investigated within this study are two types of boron-doped float-zone silicon (FZ-Si) materials with bulk resistivities of 1.1 and 3.4 Ωcm, respectively, and an initial wafer thickness of ~300 µm. Sample processing begins with an etching step using an aqueous solution of potassium hydroxide, in order to reduce the average wafer thickness to (160 ± 5) µm, as is typical for solar cells. Afterwards, the wafer surfaces are cleaned using a standard RCA sequence. As hydrogen source, silicon nitride layers (SiN_x:H) are deposited on both wafer surfaces using plasma-enhanced chemical vapour deposition (PECVD) processes either in a SiNA tool (*Meyer Burger*) or in a PlasmaLab 80 + tool (*Oxford Instruments*). The properties of the layers investigated within this study are summarized in Table 1. SiN_x:H thicknesses and refractive indices are determined using spectral ellipsometry (M2000UI, *J.A. Woollam*), the hydrogen concentration within the SiN_x:H layers is determined using Fourier-transformed infrared spectrometry (FTIR) (VERTEX 70, *Bruker*) [14,15].

Sample preparation is completed with a fast-firing step using a conventional conveyor-belt furnace (DO–FF–6.300-800, *centrotherm*). The firing conditions were set at a peak temperature of 900 °C at a belt speed of 6.8 m/min.

In order to form BH-pairs, the samples under investigation are annealed on a precision hotplate (Präzitherm TR 28-3 T, *Harry Gestigkeit*) in darkness and in ambient air at a constant temperature between 140 °C and 180 °C.

We measure the resistivity of the samples applying the eddy-current method using the sample stage of the WCT-120 lifetime tester (*Sinton Instruments*). However, instead of using the standard measurement procedure, we directly measure the output voltage of the resonant circuit (8845A, *Fluke*). Additionally, we measure the sample temperature on the measurement stage. Applying a calibration procedure, we calculate the resistivity of the sample directly from the measured difference of the output voltage of the resonant circuit and extrapolate the resistivity to a temperature of 25 °C. Please note that all resistivity values given in the following correspond to the resistivity at 25 °C. Based on this procedure and applying Gaussian error propagation we determine for the resistivity a relative uncertainty of 2.3%.

3. Results and discussion

3.1. Resistivity change due to BH pair formation

Fig. 1 shows the base resistivity of two samples upon annealing in darkness at 160 °C. Both samples feature the SiN_x:H-1 layer (see Table 1) on both wafer surfaces. While the sample corresponding to the blue circles underwent the aforementioned fast-firing step, this step was omitted for the sample corresponding to the orange squares. As can be seen from Fig. 1, if a fast-firing step is applied the resistivity changes strongly from (1.10 ± 0.03) Ωcm right after the firing process to (1.51 ± 0.03) Ωcm after annealing for 175 h at 160 °C. In contrast to this, the non-fired samples do not show any change in base resistivity. This result clearly proves that the fast-firing step is necessary to introduce significant amounts of hydrogen into the silicon bulk.

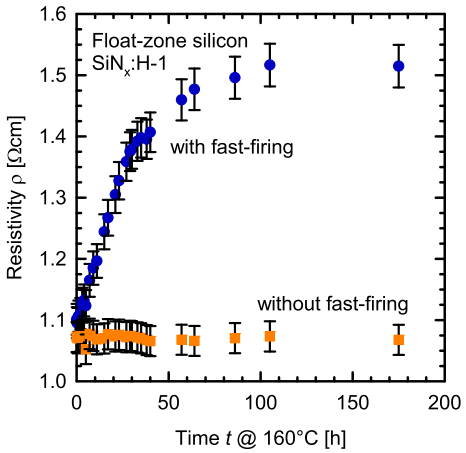

Fig. 1. Increase in the base resistivity ρ upon annealing at 160 °C, measured on a 1.1-Ωcm boron-doped FZ-Si wafer after fast-firing at a set-peak temperature of 900 °C (blue circles) and constant base resistivity of a non-fired reference sample (orange squares). Both samples feature the same silicon nitride coatings. (For interpretation of the references to colour in this figure legend, the reader is referred to the Web version of this article.)

3.2. Resistivity change depending on the applied SiNx:H layer

Fig. 2 shows the change in base resistivity of three samples upon annealing in darkness at 160 °C with the three SiN_x:H layers of different compositions (see Table 1) deposited on both wafer surfaces and fast-fired at a set-peak temperature of 900 °C. From the measured data shown in Fig. 2 it becomes clear that the change in base resistivity depends critically on the deposited film properties. While for the sample with the SiN_x:H-1 layer the resistivity changes from (3.51 ± 0.08) Ωcm to (4.08 ± 0.09) Ωcm after annealing for 90 h, the resistivity of the sample with the SiN_x:H-3 layer changes only from (3.50 ± 0.08) Ωcm to (3.67 ± 0.09) Ωcm. From the observed changes in ρ it can be concluded that SiN_x:H layers with different compositions introduce different amounts of hydrogen into the silicon bulk. An important side result is that the maximum amount of hydrogen introduced into the silicon bulk is observed for the sample featuring the lowest

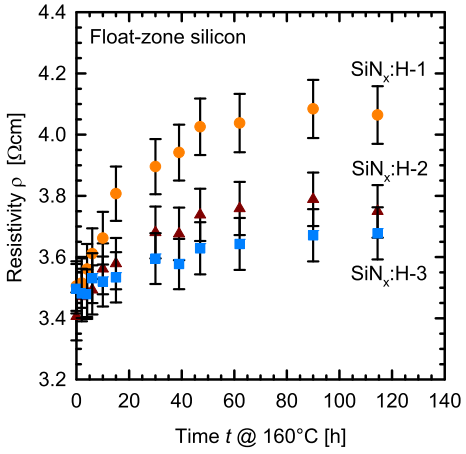

Fig. 2. Increase in base resistivity ρ upon annealing at 160 °C, measured on 3.4-Ωcm boron-doped FZ-Si wafers after fast-firing at a set-peak temperature of 900 °C. Different symbols correspond to samples with SiN_x:H layers of different compositions (see Table 1) deposited onto both surfaces. The change in base resistivity clearly depends on the composition of the SiN_x:H layers.

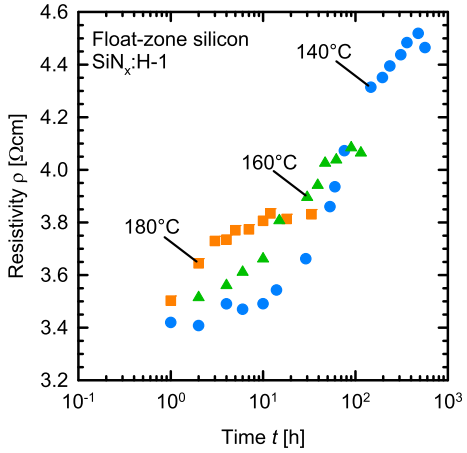

Fig. 3. Increase in base resistivity ρ upon annealing in darkness at 140 °C (blue circles), 160 °C (green triangles) and 180 °C (orange squares) measured on three samples with SiN_x:H-1 layer after fast-firing. For clarity, the uncertainty bars (2.3%) are omitted in this plot. As can be seen, the increase proceeds much slower, however to higher saturation values, at lower temperatures compared to higher temperatures. (For interpretation of the references to colour in this figure legend, the reader is referred to the Web version of this article.)

hydrogen concentration within the SiN_x:H-layer (SiN_x:H-1 layer (see Table 1). We conclude that other properties of the SiN_x:H layer than the hydrogen content determine how much hydrogen is introduced into the silicon wafer. This result is consistent with reports in the literature [16] that the mass density of the SiN_x:H layer determines the effectiveness of hydrogen in-diffusion into the silicon wafer.

3.3. Temperatur dependence of the resistivity change

Fig. 3 shows the change in base resistivity upon annealing in darkness at 140 °C, 160 °C and at 180 °C. From the time evolution of the data, it is evident that the increase in base resistivity is much faster for higher temperatures. At 180 °C, the saturation is already reached after 10 h of annealing, while at 140 °C the ρ data start to saturate only after more than 400 h. From Fig. 3 it is also notable that the saturation value of ρ increases with decreasing temperature. For annealing at 140 °C the saturation value is considerably larger than at 180 °C.

3.4. Determination of the total hydrogen concentration

According to the model of Voronkov and Falster [10], after the 'hydrogenation' via fast-firing, hydrogen is quenched-in into the silicon wafer and is mainly present in the form of hydrogen dimers H_{2A}. Note that according to the model in Ref. [10], there exist three different forms of hydrogen dimers H_{2A}, H_{2B} and H_{2C} of different configurations, which differ in their stability. Under the experimental conditions applied in this study, only one dimer configuration (namely, H_{2A}) is of relevance [10]. Upon annealing in darkness, the H_{2A} dimers gradually disappear with a simultaneous rise in the BH pair concentration. This occurs by a hole-assisted dissociation of H_{2A} into H^+ and H^0, with an immediate trapping of H^+ by boron. As the boron acceptors passivated by hydrogen no longer contribute to the samples conductivity, the concentration [BH] is experimentally easy to determine: it is equal to the difference between the hole concentration p_o (before firing) and the current hole concentration p: $[BH] = p_0 - p$. The temporal change in $[H_{2A}]$ is described by the following differential equation [10]:

$$\frac{d[H_{2A}]}{dt} = -\alpha_A\left(p \times [H_{2A}] - \chi_A \frac{([BH]/[B])^2}{p}\right) \quad (1)$$

Here, α_A is the dissociation rate coefficient of the H_{2A} dimers and χ_A is the modified equilibrium constant, depending on the equilibrium constant of the mass action laws of both contributing reactions: the hydrogen pairing ($H^0 + H^+ \leftrightarrow H_{2A} + h^+$) and the hydrogen trapping/releasing by boron acceptors ($H^+ + B^- \leftrightarrow HB$). Here [B] is the concentration of boron atoms not passivated by hydrogen: $[B] = N_B - [BH]$, with N_B the total boron concentration. The total hydrogen concentration, $[BH] + 2[H_{2A}]$ is a fixed value. The disappearance of the H_{2A} dimers leads to a simultaneous rise of BH-pairs, and the evolution of [BH] can be calculated straightforwardly using Eqn. (1). Finally, upon prolonged annealing, an equilibrium is reached between [BH] and $[H_{2A}]$. This equilibrium is according to Eqn. (1) given by

$$[H_{2A}] = \chi_A \frac{([BH]/[B])^2}{p^2} \quad (2)$$

Please note that the final equilibrium does not depend on the coefficient α_A, which only describes the temporal evolution of the BH-pair formation. Hence, from the saturated value [BH], the total hydrogen concentration can be directly determined for a given value of the equilibrium constant χ_A:

$$[H_{tot}] = 2 \times [H_{2A}] + [BH] = 2 \times \chi_A \frac{([BH]/[B])^2}{p^2} + [BH] \quad (3)$$

The hole concentration p is identical to the boron concentration [B] for non-compensated material. To validate the described model versus our experimentally determined resistivity data, we calculate the temporal formation of the BH-pairs according to Eqn. (1) and compare this with our experimentally determined formation of BH-pairs. Fig. 4 shows the evolution of the BH-pairs calculated from the measured resistivity of the fired sample in Fig. 1. The symbols show the measured data, while the solid lines correspond to the evolution of the H_{2A} and BH-pairs as calculated from Eqn. (1). Please note that for the α_A and χ_A values we took the numbers given in Ref. [10] ($\alpha_A = 10^{-21}\,cm^3s^{-1}$ and $\chi_A = 4 \times 10^{46}\,cm^9$), hence, the total hydrogen concentration $[H_{tot}]$ is the only free parameter. Comparing the solid blue line in Fig. 4 with the measurement data, we obtain an excellent agreement for the temporal evolution of [BH]. The dashed lines mark the upper and lower limits taking the uncertainties of the measurements into account. We calculate the uncertainties of [BH] using the relative uncertainties of the resistivity measurements, as mentioned above, for the measurements performed on samples with and without fast-firing. Consequently, the absolute uncertainties double and we obtain absolute uncertainties of [BH] in the range of $2 \times 10^{14}\,cm^{-3}$. These uncertainties then translate directly into the uncertainty of the total hydrogen concentration $[H_{tot}]$. For the example shown in Fig. 4 we determine a total hydrogen concentration of $[H_{tot}] = (2.85 \pm 0.15) \times 10^{15}\,cm^{-3}$.

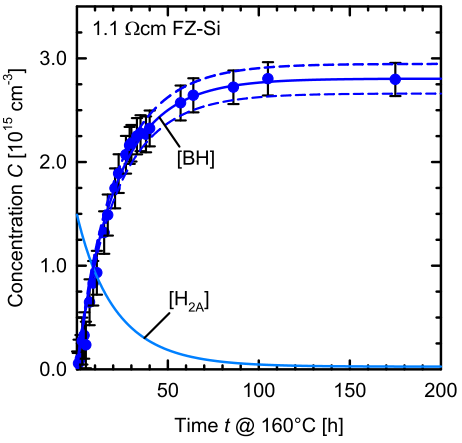

Fig. 4. Evolution of H_{2A} and BH-pairs upon annealing in darkness. Symbols correspond to [BH] calculated from the measured resistivity in Fig. 1. The solid lines are calculated according to the model. Note, the dissociation rate constant α_A and the equilibrium constant χ_A are taken from Ref. [10]. Here we determine a total hydrogen concentration of $[H_{tot}] = (2.85 \pm 0.15) \times 10^{15}\,cm^{-3}$.

Table 2
Values of the saturated BH-pair concentration $[BH]_{saturated}$ and the total hydrogen concentration $[H_{tot}]$ of the examples shown in Fig. 2. $[H_{tot}]$ is calculated according to Eqn. (3) using $\chi_A = 4 \times 10^{46}\,cm^9$.

	$[BH]_{saturated}$ [cm^{-3}]	$[H_{tot}]$ [cm^{-3}]
SiN_x:H-1	$(8.66 \pm 1.86) \times 10^{14}$	$(12.8 \pm 3.5) \times 10^{14}$
SiN_x:H-2	$(5.25 \pm 1.89) \times 10^{14}$	$(6.4 \pm 2.5) \times 10^{14}$
SiN_x:H-3	$(4.45 \pm 1.94) \times 10^{14}$	$(5.2 \pm 2.4) \times 10^{14}$

As can be seen from Fig. 2, SiN_x:H layers of different compositions lead to different magnitudes of resistivity changes. In the framework of the above model, this can be interpreted as different amounts of hydrogen being incorporated into the silicon bulk. Using the approach presented herein, we can now directly determine the total hydrogen concentration simply by determining the saturated BH-pair concentration $[BH]_{saturated}$ and calculate $[H_{tot}]$ using Eqn. (3). The results for the examples shown in Fig. 2 are given in Table 2. Again, we used a fixed value of $\chi_A = 4 \times 10^{46}\,cm^9$. Based on this analysis, we observe that the SiN_x:H layer with the lowest hydrogen concentration (10 $\%_{at.}$) introduces the highest amount of hydrogen in the silicon bulk. Hence, we can confirm that the hydrogen concentration within the layer is not an appropriate parameter describing the amount of hydrogen introduced during the fast-firing step, which is in agreement with previous studies suggesting that the mass density of the SiN_x:H layer is the most important parameter concerning the hydrogen in-diffusion into silicon during firing [16].

Within our study we investigated BH-pair formation at 160 °C on two materials with a different doping concentration, 1.1 and 3.4 Ω cm (see Figs. 1 and 2). In both cases, we analysed the samples with the SiN_x:H-1 layer (see Table 1) further as these samples feature the strongest change in base resistivity. In our analysis with regard to the dissociation coefficient α_A, we keep the modified equilibrium constant χ_A unchanged. By fitting Eqn. (1) to the measurement data, we obtain $\alpha_A = 1.6 \times 10^{-21}\,cm^3\,s^{-1}$ for the 3.4 Ω cm-material $\alpha_A = 9.6 \times 10^{-22}\,cm^3\,s^{-1}$ for the 1.1 Ω cm-material, which is in contrast to an expected fixed value of the kinetic coefficient. However, there is a simple explanation for a variation in the apparent coefficient α_A:

If, in contrast to the previous assumption, the dimers dissociate by two paths: one involving holes, $H_{2A} + h^+ \leftrightarrow H^0 + H^+$ (the rate can then be described as $\alpha_1 \times p[H_{2A}]$) and the other is a simple dissociation into neutral hydrogen, $H_{2A} \leftrightarrow H^0 + H^0$, with the corresponding rate being $\alpha_0[H_{2A}]$, then the total rate is $\gamma = (\alpha_1 \times p + \alpha_0)\,[H_{2A}]$. This means that the formally defined α_A (by a rate $\alpha_A \times p[H_{2A}]$) is an effective value equal to $\alpha_A = \alpha_1 + \alpha_0/p$, which increases towards smaller doping concentrations p.

Combining the results of the two sample types tested in the present study with the result [10] based on the work of Pritchard et al. [9] as shown in Fig. 5, first indications are that this expression for the dependence of the effective dissociation coefficient α_A on p is confirmed experimentally. A linear regression of the three data points gives rough values for the two components: $\alpha_1 = 5.8 \times 10^{-22}\,cm^3\,s^{-1}$ and $\alpha_0 = 4.3 \times 10^{-6}\,s^{-1}$ (at 160 °C).

Apart from the doping concentration, the formation of BH-pairs also critically depends on the annealing temperature. Within the previous study [10] two Arrhenius-like temperature relations for α_A and χ_A were presented. However, in light of the findings within the present study, the pre-factor in the temperature dependence of the effective dissociation coefficient α_A has to be adapted – since α_A is an effective parameter dependent on p. Taking the values for α_1 and α_0, determined at 160 °C, into account we obtain now for α_A :

$$\alpha_A = (2.3 \times 10^{-6} cm^3 s^{-1}) \times \exp\left(-1.3\frac{eV}{k_B T}\right) \quad (4)$$

The temperature dependence of the modified equilibrium constant is given by

$$\chi_A = (2.35 \times 10^{66} cm^9) \times \exp\left(-1.7\frac{eV}{k_B T}\right) \quad (5)$$

In both cases, k_B is the Boltzmann constant and T the absolute temperature.

The temperature dependence given by Eqn. (5) agrees well with our observation in Fig. 3 that a higher temperature leads to a reduction in the saturation value of [BH], since an appreciable amount of hydrogen remains non-dissociated. Additionally, as mentioned above, the evolution of the BH-pair formation does not depend on χ_A but is only characterized by the effective dissociation coefficient α_A. In order to compare our measured evolution of the BH-pair formation at the different temperatures with the predictions of the model, we use the temperature dependence given by Eqn. (5) for χ_A and fit the increase of [BH] with α_A and $[H_{tot}]$ as free parameters using Eqn. (1). Again, we used the samples with the SiN_x:H-1 layer deposited on both sides since the strongest change in base resistivity is observed on those samples. Fig. 6 shows the α_A values obtained from our data, using the mentioned fitting routine,

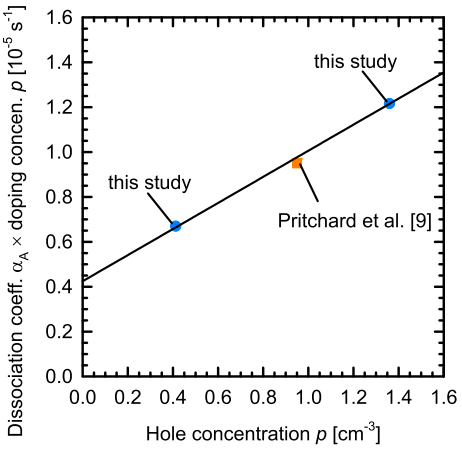

Fig. 5. Dissociation coefficient α_A multiplied with the doping concentration p plotted versus the doping concentration. Blue circles correspond to values obtained within this study. The orange square is extracted from a previous study of Pritchard et al. [9]. The linear regression (solid line) allows to easily determine the components α_1 and α_0 of the effective dissociation coefficient α_A. (For interpretation of the references to colour in this figure legend, the reader is referred to the Web version of this article.)

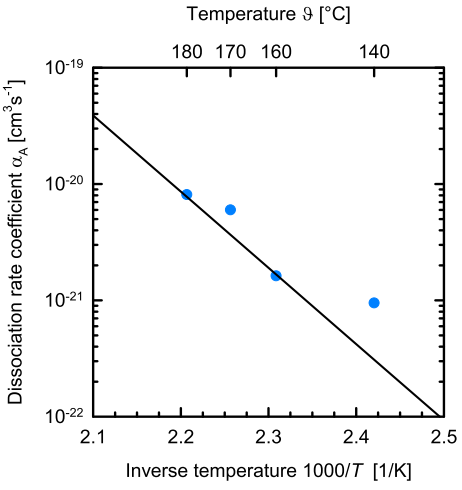

Fig. 6. Temperature dependence of the effective dissociation rate coefficient α_A. The symbols correspond to the values obtained from fitting our measurement data. The solid line gives the temperature dependence as presented within the model (see Eqn. (4)).

in comparison with the temperature dependence given by Eqn. (4). Comparing the experimental results with the result of Eqn. (4) it becomes obvious that, apart from some scattering, at temperatures between 160 °C and 180 °C, the theoretical temperature dependence agrees well with the experimental data, taking the increased pre-factor of 2.3×10^{-6} cm^3s^{-1} into account.

Finally, we address the detection limit of the presented method to determine the absolute hydrogen concentration in boron-doped silicon: The total concentration of hydrogen [H_{tot}] in a test sample is determined by measuring the saturated concentration of [BH] following an anneal and using Eqn. (3). The saturated concentration of the BH-pairs is determined by measuring the change in sample resistivity before and after a sufficiently long anneal. The detection limit is determined by the accuracy of the resistivity measurement times the hole concentration of the sample under test and the hole concentration itself which controls the fraction of the total hydrogen concentration in its detectable form [BH]. In order to detect the presence of hydrogen (initially as in the form of H_{2A}) the saturated amount of BH-pairs produced by annealing should be larger than the inaccuracy in determining p. We assume that a relative inaccuracy in p ($\Delta p/p$) is a fixed number, denoted s_p. This value is equal to the relative inaccuracy in the measured resistivity.

The total hydrogen concentration [H_{tot}] – the quantity we are interested in – is the sum of the [BH] and [H_{2A}] equilibrated contributions given by Eqn. (3) (with [B] = p). For [BH] to be larger than $\Delta p = s_p \times p$, [H_{tot}] defined by Eqn. (3) should be larger than $s_p \times p + 2\chi\, s_p^2/p^2$ which is, hence, the lower limit for detection of [H_{tot}].

Fig. 7(a) shows the lower detection limit as a function of the hole concentration p(= [B]) of a silicon wafer for two exemplary measurement accuracies for anneals at 160 °C: (i) that of the present experiment (2.3%) and (ii) an improved accuracy of 1%. In the present experiment, given a measurement uncertainty of 2.3%, the detection limits for [H_{tot}] for both investigated silicon materials are 1×10^{14} cm^{-3} and 3×10^{14} cm^{-3} for the silicon materials with base resistivities of 3.4 and 1.1 Ω cm, respectively. Because the fraction of measurable BH pairs depends on the annealing temperature through χ_A (see Eqn. (5)), the detection limit is also temperature dependent: it improves at lower annealing temperatures, as it is shown in Fig. 7(b), albeit at the expense of longer annealing times. At 140 °C, for example, given a measurement accuracy of 1%, the detection limits for [H_{tot}] would be 4.3×10^{13} cm^{-3} and 1.4×10^{14} cm^{-3} for the 3.4- and 1.1-Ω cm silicon wafers, respectively. Note that the detection limit of the technique does not decrease continuously with decreasing hole concentration of the silicon sample under investigation, but rather has a broad minimum, depending on measurement uncertainties, in the range between 10^{15} cm^{-3} and about 5×10^{15} cm^{-3} (at 160 °C). Finally, also note that any decrease in the detection limit achieved by lowering the boron concentration of the silicon sample under test will also have to be paid for with an increased annealing time required to reach saturation in [BH]. The time required is inversely proportional to the hole concentration. A test sample with a base doping concentration of 10^{15} cm^{-3} would require several weeks of annealing at 160 °C.

4. Summary

We have introduced an easy-to-apply methodology to determine the absolute hydrogen concentration within the bulk of boron-doped crystalline silicon. The method is based on recording the changes in the base resistivity of a silicon sample by contactless eddy-current measurements upon annealing in darkness at temperatures between 140 and 180 °C. Hydrogen, introduced into the silicon bulk e.g. by depositing hydrogen-rich silicon nitride and subsequent high-temperature fast-firing, binds upon annealing to the boron acceptor atoms. As these atoms no longer contribute to the sample's conductivity, the resistivity of the sample increases. Comparing the resistivity of the sample before and after hydrogenation allows the determination of the absolute concentration of BH-pairs [BH]. Applying a theoretical model presented previously, the absolute hydrogen concentration in the silicon bulk can be directly calculated from the measured resistivity changes.

The examples presented within this study already showed that in PV applications, the fast-firing process is necessary to introduce hydrogen in relevant amounts from a hydrogen-rich silicon nitride layer (SiN_x:H) into the silicon bulk. Additionally, the composition of the SiN_x:H layer is of major importance, as SiN_x:H layers of different compositions introduce different amounts of hydrogen. Within the examples shown here, a SiN_x:H layer with a hydrogen concentration of 10 $\%_{at.}$ introduced a total hydrogen concentration of [H_{tot}] = 1.3×10^{15} cm^{-3} into the silicon bulk, whereas a layer of the same thickness but with a hydrogen concentration of 13 $\%_{at.}$ introduced only [H_{tot}] = 4.5×10^{14} cm^{-3}, clearly demonstrating that it is not the hydrogen content of the SiN_x:H layer that determines the amount of hydrogen introduced into the silicon bulk.

Finally, we have also examined the doping and temperature dependence of the BH-pair formation. Our results presented here support the idea that the previously neglected dissociation path of the hydrogen dimers by thermal dissociation into neutral hydrogen atoms also plays a relevant role for the formation of BH-pairs. Hence we conclude that the dissociation coefficient α_A of the H_{2A} dimers is in fact an effective dissociation coefficient of the form $\alpha_A = \alpha_1 + \alpha_0/p$, with α_1 being the dissociation coefficient of the hole assisted dissociation process and α_0 being the dissociation coefficient of the dissociation process into neutral hydrogen atoms. This is an important modification of the conversion mechanism between H_{2A} and BH.

Acknowledgement

This work was partly funded by the state of Lower Saxony and the German Federal Ministry of Economics and Energy (BMWi) within the

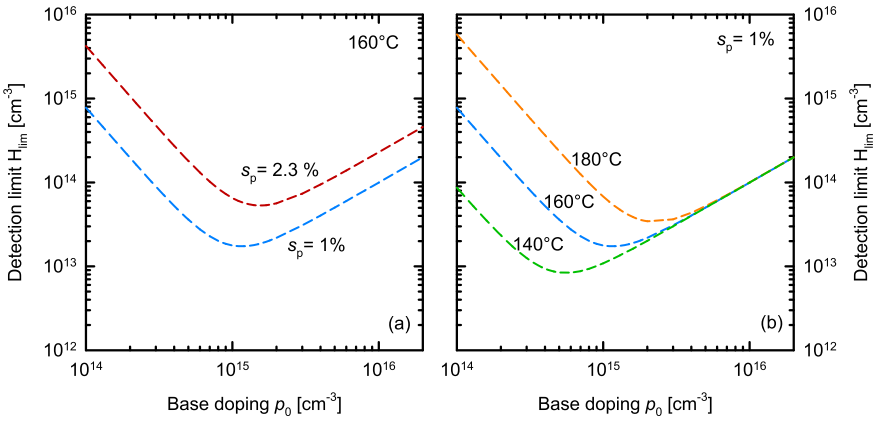

Fig. 7. (a) Calculated detection limit of the absolute hydrogen concentration [H_{lim}] as a function of the bulk doping concentration p_0 of a silicon sample for two different relative uncertainties of the resistivity measurement s_p and for an annealing at 160 °C. The measurements presented in this paper have an uncertainty of s_p = 2.3% (red dashed line). (b) Calculated dependence of [H_{lim}] as a function of p_0 for different annealing temperatures and a fixed relative uncertainty of s_p = 1%. (For interpretation of the references to colour in this figure legend, the reader is referred to the Web version of this article.)

research project “LIMES” (contract no. 0324204D). The content is the responsibility of the authors.

References

[1] A.G. Aberle, Overview on SiN surface passivation of crystalline silicon solar cells, Sol. Energy Mater. Sol. Cell. 65 (1–4) (2001) 239–248.

[2] F. Jiang, M. Stavola, A. Rohatgi, D. Kim, J. Holt, H. Atwater, J. Kalejs, Hydrogenation of Si from SiNx(H) films: characterization of H introduced into the Si, Appl. Phys. Lett. 83 (5) (2003) 931–933.

[3] B.L. Sopori, X. DENG, J.P. Benner, A. Rohatgi, P. SANA, S.K. Estreicher, Y.K. Park, M.A. Roberson, Hydrogen in silicon: a discussion of diffusion and passivation mechanisms, Sol. Energy Mater. Sol. Cell. 41–42 (1996) 159–169.

[4] F. Duerinckx, J. Szlufcik, Defect passivation of industrial multicrystalline solar cells based on PECVD silicon nitride, Sol. Energy Mater. Sol. Cell. 72 (1–4) (2002) 231–246.

[5] Hydrogen passivation of multicrystalline silicon, in: C.E. Dube, J.I. Hanoka (Eds.), Photovoltaic Specialists Conference, Conference Record of the Thirty-first IEEE, 20052005.

[6] A.G. Aberle, Surface passivation of crystalline silicon solar cells: a review, Prog. Photovoltaics Res. Appl. 8 (5) (2000) 473–487.

[7] J. Schmidt, M. Kerr, A. Cuevas, Surface passivation of silicon solar cells using plasma-enhanced chemical-vapour-deposited SiN films and thin thermal SiO 2/ plasma SiN stacks, Semicond. Sci. Technol. 16 (3) (2001) 164–170.

[8] F.A. Stevie, C. Zhou, M. Hopstaken, M. Saccomanno, Z. Zhang, A. Turansky, SIMS measurement of hydrogen and deuterium detection limits in silicon: comparison of different SIMS instrumentation, J. Vacuum Sci. Technol. B, Nanotechnol. Microelectron.: Mater. Process. Measure. Phenomena 34 (3) (2016) 03H103.

[9] R.E. Pritchard, J.H. Tucker, R.C. Newman, E.C. Lightowlers, Hydrogen molecules in boron-doped crystalline silicon, Semicond. Sci. Technol. 14 (1) (1999) 77.

[10] V.V. Voronkov, R. Falster, Formation, dissociation, and diffusion of various hydrogen dimers in silicon, Phys. Status Solidi (b) (2017) 1600779.

[11] C. Herring, N.M. Johnson, Van de Walle, G. Chris, Energy levels of isolated interstitial hydrogen in silicon, Phys. Rev. B 64 (12) (2001) 125209.

[12] S.J. Pearton, J.W. Corbett, T.S. Shi, Hydrogen in crystalline semiconductors, Appl. Phys. A 43 (3) (1987) 153–195.

[13] J.I. Pankove, R.O. Wance, J.E. Berkeyheiser, Neutralization of acceptors in silicon by atomic hydrogen, Appl, Phys. Lett. 45 (10) (1984) 1100–1102.

[14] W.A. Lanford, M.J. Rand, The hydrogen content of plasma-deposited silicon nitride, J. Appl. Phys. 49 (4) (1978) 2473.

[15] Z. Yin, F.W. Smith, Optical dielectric function and infrared absorption of hydrogenated amorphous silicon nitride films: experimental results and effective-medium-approximation analysis, Phys. Rev. B 42 (6) (1990) 3666–3675.

[16] A.W. Weeber, H.C. Rieffe, W.C. Sinke, W.J. Soppe, Structural and Passivating Properties of SiNx:H Deposited Using Different Precursor Gases, Proc. 19th EUPVSEC, Paris, France, 2004, pp. 1005–1008.